CONCRETE LIBRARY OF JSCE NO.18, DECEMBER 1991

DETERMINATION OF TENSION SOFTENING DIAGRAMS OF CONCRETE BY MEANS OF BENDING TESTS

(Reprint from Proceedings of JSCE, No.426/V-14, Feb. 1991)

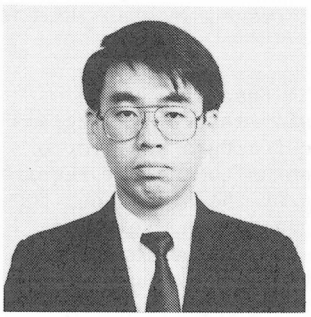

Yuichi UCHIDA

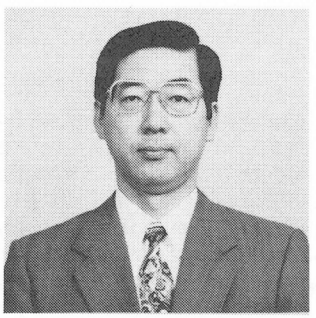

Keitetsu ROKUGO

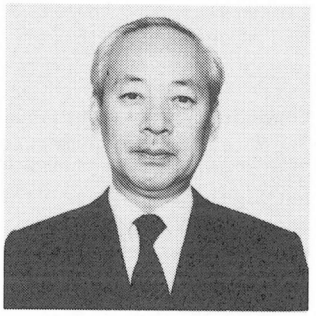

Wataru KOYANAGI

SYNOPSIS

A simple and handy test method for determination of the tension softening diagrams of concrete from bending tests on notched beams is proposed. This method has the following features: (1) the tension softening diagram can be determined from a single beam specimen, (2) the method can be combined with the RILEM method for determination of the fracture energy G_F, (3) only the load, the loading point displacement and the notch tip opening are necessary to be measured, (4) the second derivative of the potential energy is introduced to improve the accuracy of the estimation of the diagrams. The proposed method is applied to various kinds of concrete including high strength concrete and light weight concrete to determine the diagrams and also to certify the validity of the method.

Y. Uchida is now research associate of civil engineering at Gifu University, Gifu, Japan. Previously, he was research engineer at Research Institute of Shimizu Construction Co., LTD, Japan. He received his Master of Engineering Degree in 1983 from Gifu University. His current research interests include the numerical analysis and the fracture mechanics of concrete. He is a member of JSCE, JCI and ACI.

K. Rokugo is associate professor of civil engineering at Gifu University. He received his Doctor of Engineering Degree in 1980 from Kyoto University. He is a secretary of JCI Committee on the fracture mechanics of concrete. His research work covers the failure behavior of concrete and reinforced concrete members. He is a member of JSCE, JCI, ACI, RILEM and CEB.

W. Koyanagi is professor of civil engineering at Gifu University and member of the administrative council of the university. He received his Doctor of Engineering Degree in 1977 from Kyoto University. His research interests cover the fracture behavior of concrete materials, reinforced concrete members and structures, the structural design method and the application of new building materials. He is a member of JSCE, JSMS, JCI and ACI.

---

1. INTRODUCTION

As well as the strength properties of concrete, additional material properties such as the fracture energy and the tension softening diagram have been needed for precise prediction of the failure behavior of important concrete structures through numerical analyses. The fracture of concrete due to cracks is distinguished by the so-called fracture process zone (FPZ) in front of the tip of the opened crack [1]. FPZ is the nonlinear region where many microcracks are accumulated. In the FPZ the transferred stress decreases with an increase in the tensile strain (or total crack opening).

Research activities are progressing in the field of the Fracture Mechanics of Concrete, where the fracture energy G_F and the tension softening diagrams are applied to the numerical analysis to deal with the fracture behavior of concrete structures. The fracture energy G_F is defined as the energy required to propagate a tensile crack of unit area and is given by the area under the tension softening diagram. The tension softening diagram is the relation between the decreasing transferred tensile stress and the increasing tensile strain or crack opening in the FPZ. The establishment of the measuring method of the tension softening diagrams is one of the important subjects in Fracture Mechanics of Concrete, in addition to the investigations on the phenomena in the FPZ, the size-dependent properties of concrete strengths, the evaluation of fracture behavior and so on [1].

The standardized testing method to determine the fracture energy G_F of concrete by means of three point bending tests on notched beams has been proposed by RILEM [2]. On the other hand, the testing method to determine the tension softening diagrams has not been standardized, because it is generally not easy to measure the post-peak curves in the direct tension tests. The following methods have been proposed: (a) direct tensile test using stiff testing machine [3], (b) data fitting techniques to solve an inverse problem [4], (c) multi-cutting technique [5], and so on. These methods and techniques are still not easy to perform even in well-equipped laboratories.

The J-integral based method for the determination of the tension softening diagrams from bending tests on notched beams proposed by Li et al. [6] and the simplified new J-integral based method [7] seem to be practical and easy methods, which require no special equipments, although the accuracy of the methods should be improved.

In this contribution, the **Li's J-integral based method** and the **new J-integral based method** are described and then a **modified J-integral based method** is proposed. The tension softening diagrams of plain concrete, high strength concrete and light weight concrete are determined through the proposed modified method. The validity of the method is examined by comparison of numerical and experimental results.

2. TENSION SOFTENING DIAGRAMS AND LOAD-DISPLACEMENT CURVES OF NOTCHED BEAMS

The macro crack propagating process can be simulated through FEM and BEM with the fictitious crack model [1], where the crack in the FPZ is expressed by the separation of the nodes and the closing force (transferred tensile force) depending on the crack opening is introduced between the nodes. This model is effective when a main crack governs the failure behavior and enables us to analyze the descending region of members after the peak load. In this chapter the effects of the tension softening properties on the load-displacement curves of the notched concrete beams are investigated through FE-analysis with

the fictitious crack model.

Fig. 1 shows the finite element mesh of the left hand side of the specimen, which is 10x10x84 cm (loading span: 80 cm) and has a 5 cm notch (half of the specimen depth) at the bottom center. This size and shape of the specimen are equal to those specified in the RILEM testing method for G_F. Fig. 2 indicates three typical tension softening diagrams, which are the 1/4 bilinear model [8], the -3 power model [9] and the linear model. In the 1/4 bilinear model the stress at the turning point is 1/4 of the tensile strength.

Fig. 3 shows the effects of the tensile strength f_t on the simulated load-displacement curves of the beams. The tensile strength f_t was chosen to be 20, 35, and 50 kgf/cm^2 and the -3 power model was adopted with the constant G_F value of 0.15 kgf/cm. The maximum load increases with an increase in the tensile strength. As indicated in Fig. 3, however, the ratio of the flexural strength to the tensile strength (f_b/f_t) decreases as f_t increases. Here f_b means the value calculated by dividing the maximum moment by the section modulus.

Fig. 4 shows the effects of the G_F value on the load-displacement curves. The tensile strength f_t was 35 kgf/cm^2 and the -3 power model was used. The G_F value of 0.05 kgf/cm implies the one for light weight concrete. The value for normal plain concrete is 0.10 ∿ 0.15 kgf/cm. The maximum flexural load increases remarkably as the G_F value increases.

The effects of the shape of the tension softening diagrams on the load-displacement curves are shown in Fig. 5. The maximum flexural load and the curve shape in the case of the linear model are different from those for the 1/4 bilinear model and the -3 power model. Therefore, the shape of the tension softening diagrams is important for the numerical prediction of the failure

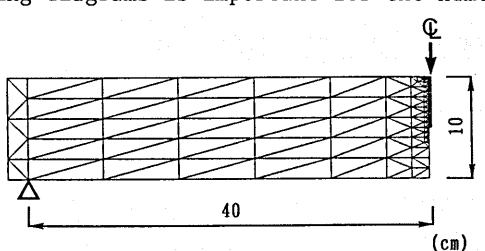

Fig. 1 Finite element mesh.

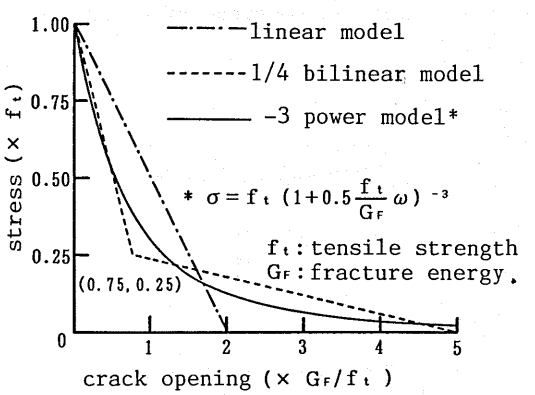

Fig. 2 Tension softening models.

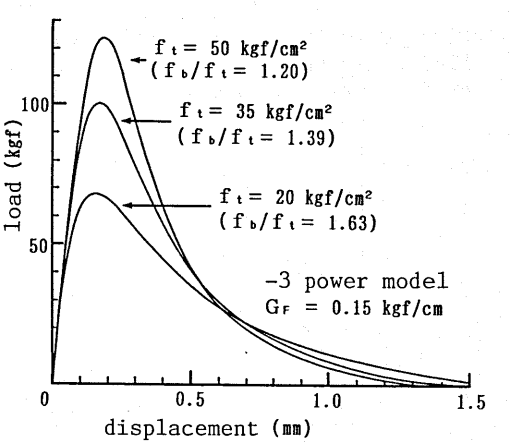

Fig. 3 Effect of tensile strength on load-displacement curves.

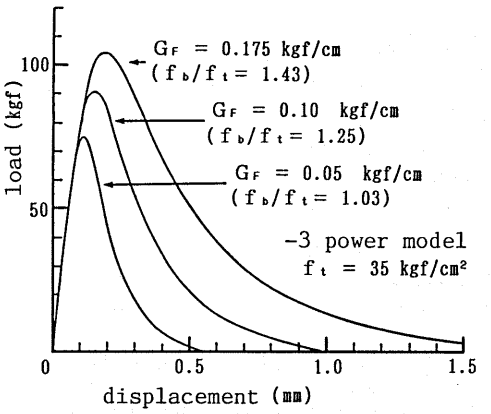

Fig. 4 Effect of fracture energy on load-displacement curves.

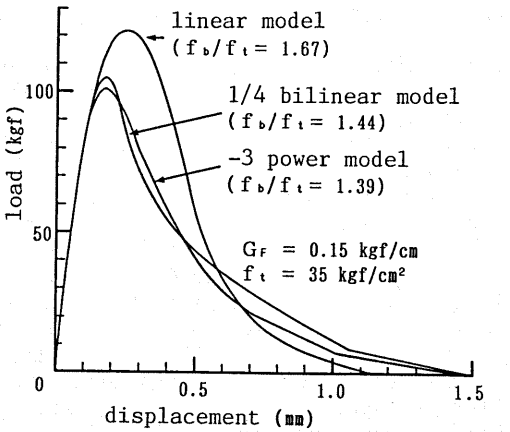

Fig. 5 Effect of shape of model on load-displacement curves.

behavior of concrete members. Since the 1/4 bilinear model and the -3 power model give simulated curves having the similar shape, the simpler bilinear model seems to be enough for the numerical simulation.

It can be concluded from these numerical results that not only the tensile strength but also the G_F value and the shape of the softening diagrams have effects on the failure behavior of concrete members due to cracks. Therefore, the testing method for determination of the tension softening properties such as the shape of the diagrams and G_F value should be standardized.

3. METHODS FOR DETERMINATION OF TENSION SOFTENING DIAGRAMS

3.1 Principle of determination of tension softening diagrams from bending tests

The tension softening diagram is given by the following equation:

$$\sigma = \sigma(\omega) \tag{1}$$

where, σ is the tensile stress and ω is the crack opening (width). As illustrated in Fig. 6, when the crack opening reaches ω the required energy per unit crack area $e(\omega)$ is given by the area under the tension softening

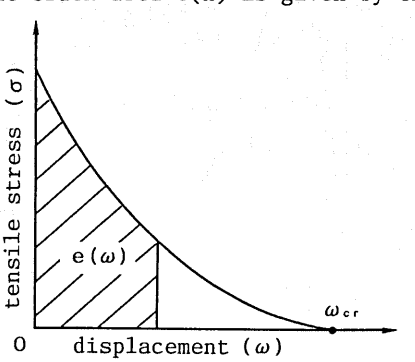

Fig. 6 Tension softening diagram and consumed energy.

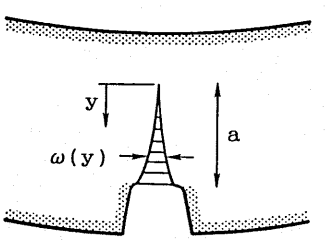

Fig. 7 Notch tip.

diagram and hence is expressed as:

$$e(\omega)=\int_0^{\omega}\sigma(\omega)d\omega \tag{2}$$

At the complete crack opening ω_{cr}, the transferred stress becomes zero and $e(\omega_{cr})$ coincide with the fracture energy G_F. It is seen from eq.(2) that $\sigma(\omega)$ can be determined from the derivative of $e(\omega)$ with respect to ω, if $e(\omega)$ is measured in experiments. That is:

$$\sigma=\sigma(\omega)=\frac{de(\omega)}{d\omega} \tag{3}$$

As shown in Fig. 7, the total energy E consumed in the cracked region until the crack length becomes a, is given by the following equation, by integrating $e(\omega)$ in the crack direction:

$$E=b\cdot\int_0^{a}e(\omega(y))dy \tag{4}$$

where $\omega(y)$ is the distribution function of the crack opening and b is the specimen width. Therefore, if E, a, and $\omega(y)$ are measured in experiments, $e(\omega)$ is given and then the tension softening diagram $\sigma(\omega)$ can be determined.

3.2 Li's J-integral based method

As illustrated in Fig. 8, the Li's J-integral based method [6] uses $e(\omega)$ obtained from E, a, and $\omega(y)$ in eq.(4), which are assumed or measured during loading tests of two beam specimens having slightly different notch lengths ($n_1<n_2$). In the J-integral method, $e(\omega)$ is the J-integral value, and the crack length a is the difference in the notch lengths ($a=n_2-n_1$). The total energy E consumed in the cracked region is given by the difference in the areas of the load-displacement curves ($P_1(\delta)$, $P_2(\delta)$). The distribution of the crack opening is assumed to be uniform for the small crack length a. The crack opening ω is taken to be the average of the measured crack openings w_1 and w_2 at the notch tip ($\omega=(w_1+w_2)/2$). From eq.(4):

$$e(\omega)=E(\omega)/(b\cdot a) \tag{5}$$

where $\omega=\omega(\delta)=(w_1(\delta)+w_2(\delta))/2$, $a=n_2-n_1$, and $E(\omega)=E(\omega(\delta))=\int_0^{\sigma}(P_1(\delta)-P_2(\delta))d\delta$.

The tension softening diagram can be determined by differentiating eq.(5).

The Li's J-integral based method is accurate in the numerical calculation but

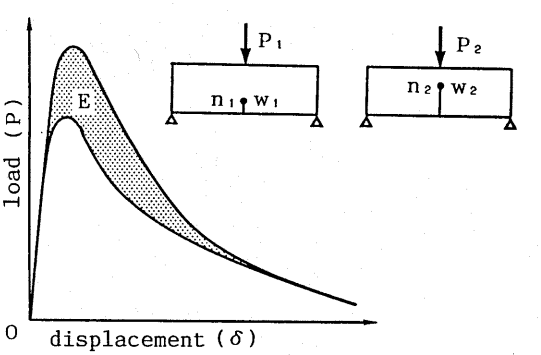

Fig. 8 Li's J-integral based method.

sensitive to the scatter in the experimental data [10], because this method uses the total energy E measured from the difference of the curves of two specimens. This is the disadvantage of the Li's method.

3.3 New J-integral based method

We have proposed our new J-integral based method to determine tension softening diagrams from a single specimen by simplifying the Li's method [7]. A virtual specimen with a full notch length (without ligament) is used instead of one of the two specimens required in the Li's method. This new J-integral based method is discussed in this session.

In the new method, the crack length a is the ligament length a_0, that is $a=a_0$. The crack opening ω is a half of the notch tip opening w of the actual specimen ($\omega=w/2$), because the notch tip opening of the virtual specimen is zero. The total energy E is the area under the load-displacement curve of the actual specimen. This means that the energy applied to the specimen is consumed in the cracked region. Therefore, eq.(4) becomes:

$$E(\omega)=A_{lig}\cdot e(\omega) \tag{6}$$

where A_{lig} is the ligament area (ba_0).

The total energy E until the notch tip opening reaches w is given as:

$$E(\omega)=\int_0^{\delta_w} P(\delta)d\delta \tag{7}$$

where δ_w is the loading point displacement when the notch tip opening is w. $e(\omega)$ is given as:

$$e(\omega)=1/A_{lig}\cdot\int_0^{\delta_w} P(\delta)d\delta \tag{8}$$

The load-displacement curve $P(\delta)$ in eq.(7) is corrected to eliminate the effect of the specimen's weight, that is, a half of the specimen's weight is added to the load value.

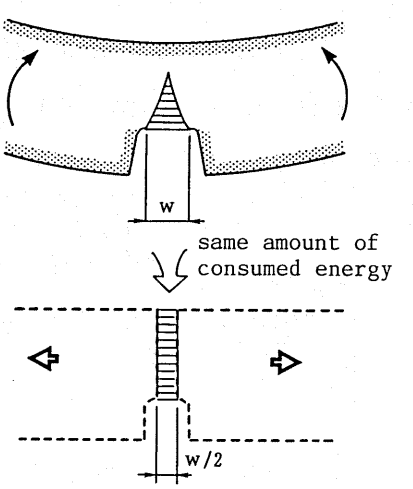

Fig. 9 Modeling of new J-integral based method.

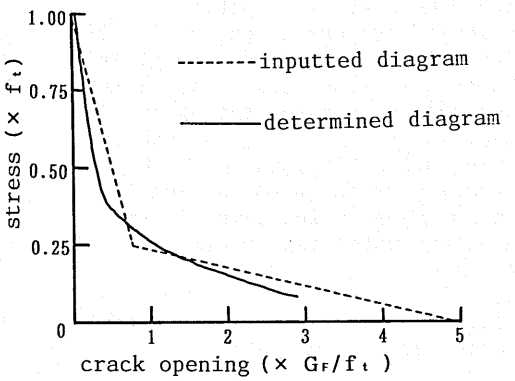

Fig. 10 Determination of bilinear softening diagram through new J-integral based method.

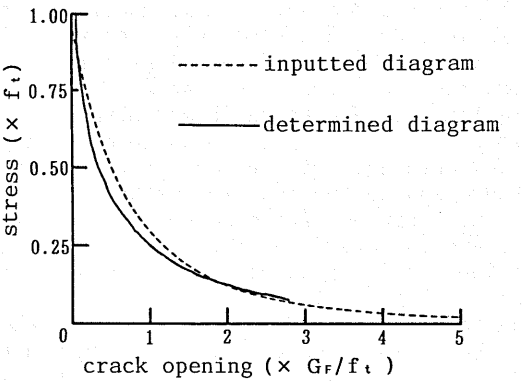

Fig. 11 Determination of power softening diagram through new J-integral based method.

Fig. 9 illustrates the concept of the new J-integral based method. The beam specimen is replaced by the imagined uniaxial tension specimen, where the crack opening ω is a half of the notch tip opening w and the non-cracked region is rigid.

This new method was examined through numerical analysis and the results are shown in Figs. 10 and 11. The bilinear model and the power model shown in Fig. 2 were used for the simulation of load-displacement curves of notched beams (size and mesh are shown in Fig. 1), and then the tension softening diagrams were determined through the new method. The inputted diagrams and the determined ones are given in Figs. 10 and 11. The stress of the determined diagrams for the small crack opening is lower than that of the inputted diagrams. In the case of the bilinear diagram, the turning point moves to the upper and left side. There is a gap between tensile strengths of the inputted and the determined diagrams. These differences may be caused due to the following reasons. The compression zone and the non-cracked zone are ignored. The energy stored in the elastic region is not considered. The crack opening is assumed to be a half of the notch tip opening and the distribution is uniform.

The new J-integral based method, however, gives softening diagrams not sensitive to the scatter in experimental data. Therefore, this method is effective for rough estimation of softening diagrams and for comparative studies on different kinds of concrete. This method can be combined with the RILEM testing method for G_F.

3.4 Modified J-integral based method

The assumptions introduced for the above new J-integral based method are summarized as follows:

1) The crack length is the ligament length.
2) The energy applied to the specimen is consumed in the cracked region.
3) The crack opening is a half of the notch tip opening and the distribution is uniform.

These three assumptions cause errors in the shape of the determined softening diagrams. In this session, therefore, we improve the new J-integral based method to determine the softening diagrams more precisely. The improved one is called the modified J-integral method.

Only the third assumption is modified and the others are left without modification. Since the experimental detection of the crack length is difficult and the separation of the elastic strain energy from the applied energy is also not easy, the first and the second assumptions are not changed. In the previous new J-integral based method, the deformation due to bending is simplified as that due to uniform tension as illustrated in Fig. 9, and the crack opening ω is supposed to be a half of the notch tip opening w. On the other hand in the modified method, the deformation of the beam is idealized as the rotation with a center on the compression edge as indicated in Fig. 12, and the crack opening ω is the function of the notch tip opening w. This is the modification of the third assumption.

The total energy E consumed in the cracked region until the notch tip opening reaches w is given by eq.(4), using the relation of $\omega(y)=w\cdot y/a_0$:

$$E(w)=\frac{A_{11g}}{w}\int_0^w e(w)dw \tag{9}$$

From eq.(3) and the second derivative of eq.(9) with respect to w, the following equation can be obtained:

$$\sigma(w)=(wE''(w)+2E'(w))/A_{11g} \tag{10}$$

The total energy E (applied energy to the specimen) until the notch tip opening reaches w is given as:

$$E(w)=\int_0^{\sigma_w} P(\delta)d\delta \tag{11}$$

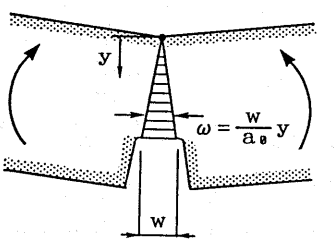

Fig. 12 Modeling of modified J-integral based method.

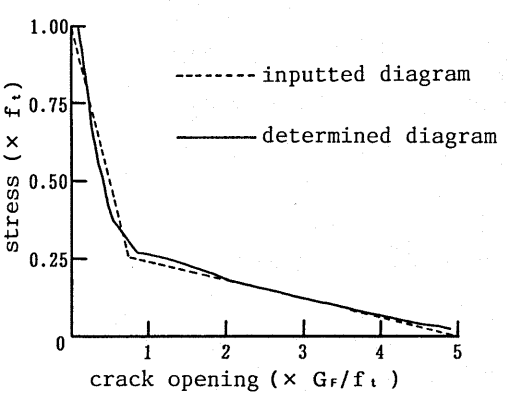

Fig. 13 Determination of bilinear softening diagram through modified J-integral based method.

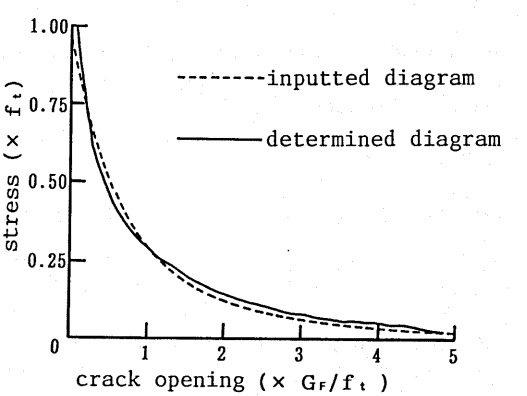

Fig. 14 Determination of power softening diagram through modified J-integral based method.

where δ_w is the loading point displacement when the notch tip opening is w.

$\sigma(w)$ is derived from eqs.(10) and (11) and then the tension softening diagram is obtained by replacing w with ω. The load-displacement relation $P(\delta)$ in eq.(11) is corrected in the load value by adding a half of the specimen's weight.

The accuracy of the modified method is examined through FE-analysis using the 1/4 bilinear model and the -3 power model. Figs. 13 and 14 show the inputted softening diagrams (dotted line) and the determined diagrams (solid line) through the modified method. It is seen that the modified method gives more precise results (Figs. 13 and 14) than the new method (Figs. 10 and 11).

The tensile strength (softening initiation stress) can not be exactly determined even through the modified method. The reasons are that the crack length is taken to be the ligament length and the elastic energy stored in non-cracked region is ignored. Since eq.(10) includes the first and the second derivatives of E(w), smooth E(w) values are necessary for the numerical derivative operations. Especially at the beginning part of the diagram the absolute value of E(w) is so small that the shape of the diagram tends to be sensitive to the scatter of the data. Therefore, the tensile strength (softening initiation stress) of the diagram, even if it is determined through the modified method, should be adjusted to the tensile strength measured from standard tests such as splitting tests. Practical procedures for the adjustment are described in the next chapter.

The next topic is to discuss the reason why the modified method can predict reasonable shapes of the softening diagrams except for the initial part, in spite of the first assumption of the crack length and the second assumption of the elastic energy. In Fig. 15, the ratio of crack length to the ligament length (a/a_0) and the ratio of the total energy to the consumed energy at cracked region (E_T/E_F) are plotted with the notch tip opening for the case of the numerical simulation shown in Fig. 3, where the tensile strength f_t is chosen to be 35 kgf/cm^2 for typical concrete. The ratio a/a_0 indicates the degree of the underestimation of $e(\omega)$ due to the first assumption that the crack length is equal to the ligament length. The ratio of E_T/E_F represents the degree of the overestimation of $e(\omega)$ due to the second assumption that the elastic energy is ignored. Their product $(a/a_0)\cdot(E_T/E_F)$ may indicates the degree of the deviation of $e(\omega)$ from the true value. As seen from Fig.

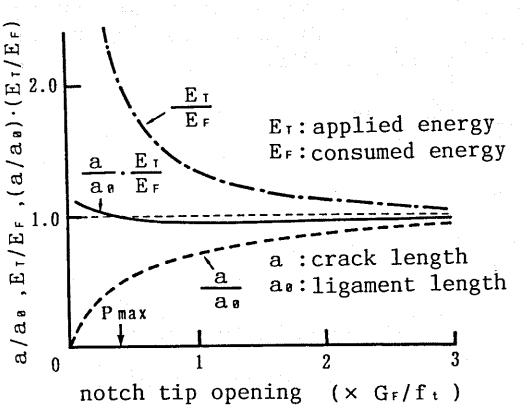

Fig. 15 Effects of crack length and elastic energy on $e(\omega)$.

15, though the product $(a/a_0)\cdot(E_T/E_F)$ slightly deviates at the beginning part, the value remains about 1.0 after the peak load (P_{max}) and the errors introduced by the two assumptions compensates with each other. The assumption on the crack length causes the underestimation of $e(\omega)$, which is the energy consumed in the actual cracked region, and the ignorance of the elastic energy causes the overestimation. Both errors compensate with each other and hence there are small effects on the determined shape of the diagrams except for the beginning part.

4. MEASUREMENTS OF TENSION SOFTENING DIAGRAMS OF VARIOUS KINDS OF CONCRETE

4.1 Outline of experiments

The tension softening diagrams were determined through the modified J-integral based method for plain concrete at different loading ages, for high strength concrete, and for light weight concrete. The loading tests were performed according to the RILEM testing method [2] and the fracture energy G_F was measured. The plain concrete was tested in wet condition at ages of 3 days, 7 days, and 28 days. The water-cement ratio (W/C) of the high strength concrete was 0.27 and superplastisizer was used. The weight of unit volume was 1.63 t/m^3 for the light weight concrete, where artificial light weight sand and coarse aggregates were adopted. Specimens made of the high strength concrete and the light weight concrete were cured for two weeks in wet condition and then placed in a testing room for eight weeks until loading tests.

The size of the specimens was 10x10x84 cm and the loading span was 80 cm. The notch length was 5 cm, which is a half of the specimen depth. Notches were made using a concrete cutter. The width of the notch was about 5 mm. Five or six specimens were loaded for each testing condition.

The setup of the bending test is shown in Fig. 16. The applied load, the beam displacement at center, and the notch tip opening were measured. The gauge length for the notch tip opening measurement was 3 cm. The elastic deformation inside this gauge length was ignored, because the deformation would be enough small as compared with the notch tip opening. Rollers were used under the supports to eliminate the restriction in the horizontal direction. The settlement at the supports was eliminated from the measured beam center deflection (displacement). The loading time from the beginning to the peak load was about one minute or less. A conventional testing machine without a servo-controller was used. Loading and unloading operations were performed so as to prevent a sudden failure after the peak load.

4.2 Test results and discussions

Tests results are tabulated in Table 1. Measured load-displacement curves

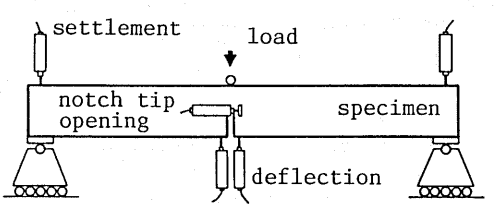

Fig. 16 Three-point bending test.

are shown in Figs. 17 to 21, where the shaded area indicates the scatter band of the curves. The fracture energy G_F of the light weight concrete was about 1/3 of that of the plain concrete, because of the weak coarse aggregate. The G_F value of the high strength concrete was only 10% greater than that of the plain concrete, though the compressive strength was about twice. The increase in the flexural strength of the plain concrete with age was small as compared with the increase in both the compressive strength and the tensile strength. This can be explained by the small increase in G_F with age.

Fig. 22 shows the tension softening diagram of the plain concrete at the age of 28 days, which was determined through the modified J-integral based method. The tensile strength of the determined diagram (stress at zero opening) is different from the tensile strength from splitting tests. The peak point of the diagram is not on the stress axis. In this investigation, we recommend to replace the beginning part of the diagram by the tangential line starting

Table 1 Properties of concrete.

Concrete	Strength (kgf/cm²)			Fracture energy G_F (kgf/cm)
	Compressive	tensile	flexural	
High strength conc.	848	53.0	75.7	0.178
Light weight conc.	344	22.3	30.1	0.053
Plain conc., 3 days	195	17.6	38.2	0.134
Plain conc., 7 days	292	26.7	46.6	0.144
Plain conc., 28 days	407	34.3	50.5	0.160

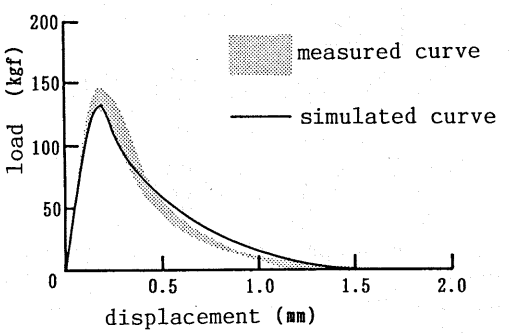

Fig. 17 Load-displacement curves of high strength concrete beams.

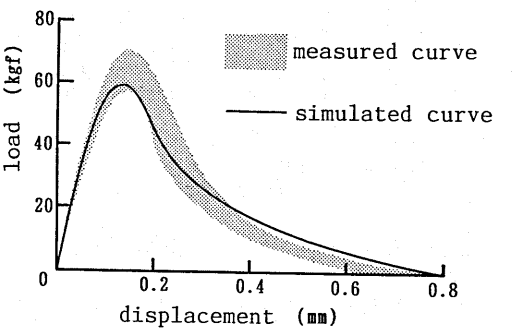

Fig. 18 Load-displacement curves of light weight concrete beams.

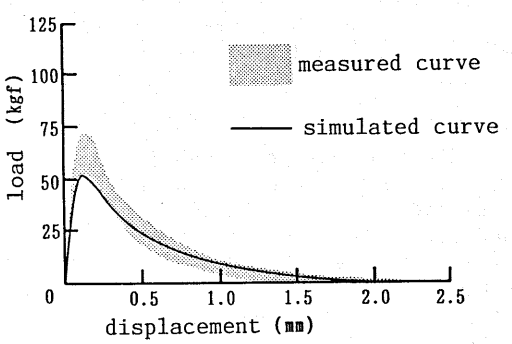

Fig. 19 Load-displacement curves of plain concrete at 3 days.

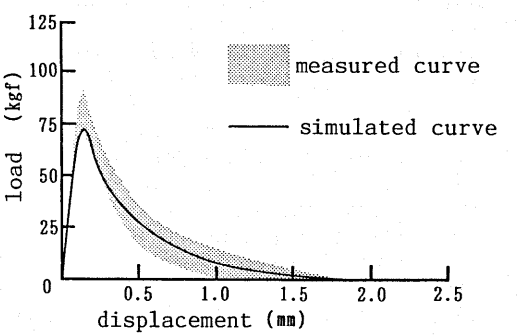

Fig. 20 Load-displacement curves of plain concrete at 7 days.

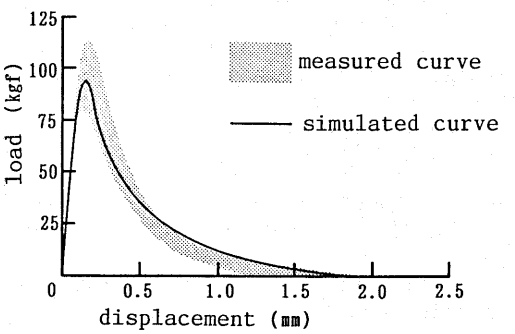

Fig. 21 Load-displacement curves of plain concrete at 28 days.

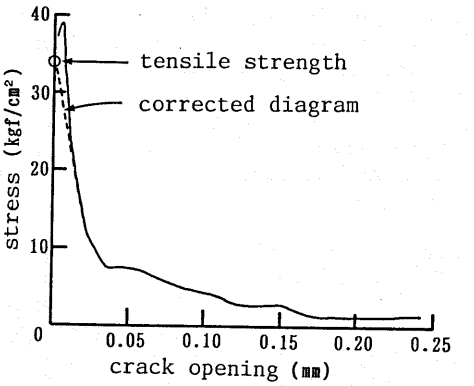

Fig. 22 Correction of determined tension softening diagrams.

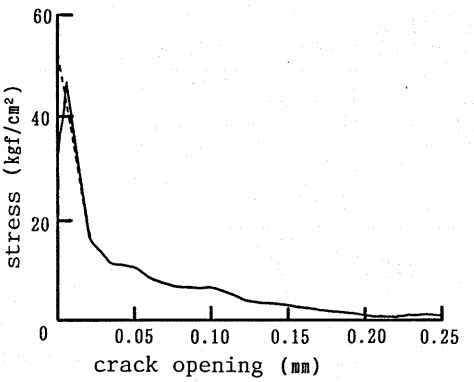

Fig. 23 Tension softening diagram of high strength concrete.

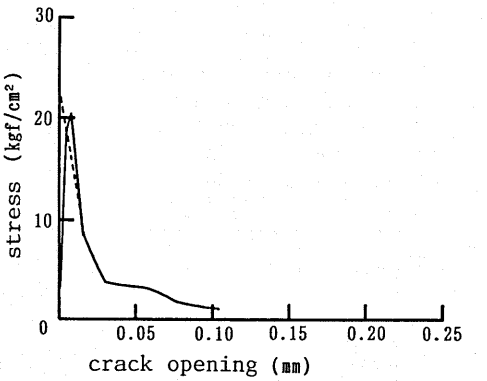

Fig. 24 Tension softening diagram of light weight concrete.

from the splitting tensile strength (dotted line), because the tensile strength of the diagram (the softening initiation stress) has greater effects on results of numerical analysis than the shape of the diagram.

The tension softening diagrams of various kinds of concrete were determined through the modified J-integral based method and are shown in Fig. 23 to 27, together with the tangential lines mentioned above (dotted line). Fig. 28 shows the normalized diagrams, where the vertical and horizontal axes are σ/f_t and $\omega \cdot f_t/G_F$, respectively. The shapes of the normalized diagrams are similar with each other and are close to the 1/4 bilinear model and the -3 power model.

The load-displacement curves of beam specimens were simulated through FE-analysis using the determined softening diagrams and are shown in Figs. 17 to 21 with a solid line. In the analysis, the measured softening diagrams were approximated with 4 to 7 line segments and the complete crack openings (where no stress transfer) were determined so as the area under the diagram became the fracture energy G_F. The Young's moduli were determined from the initial slope of the measured load-displacement curves. The simulated load-displacement curves are in good accordance with the measured ones. Therefore, it is seen that the softening diagrams determined through the modified J-integral based method are reasonable and that the method is effective.

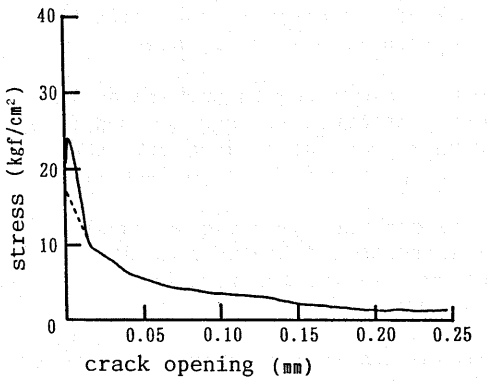

Fig. 25 Tension softening diagram of plain concrete at 3 day.

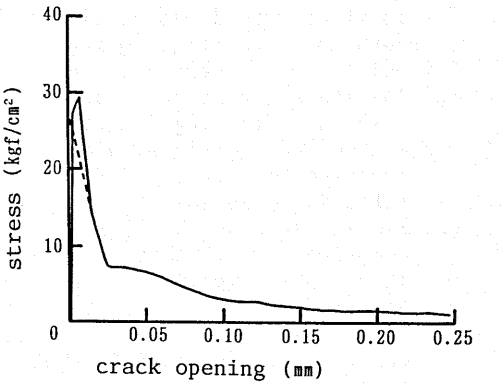

Fig. 26 Tension softening diagram of plain concrete at 7 days.

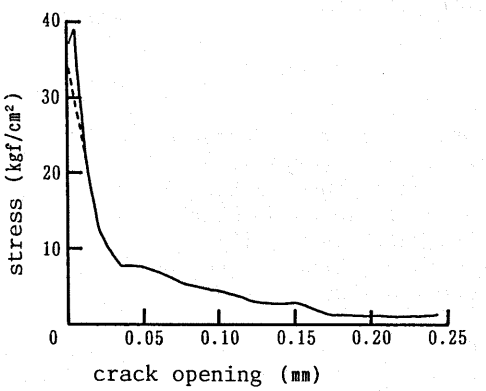

Fig. 27 Tension softening diagram of plain concrete at 28 days.

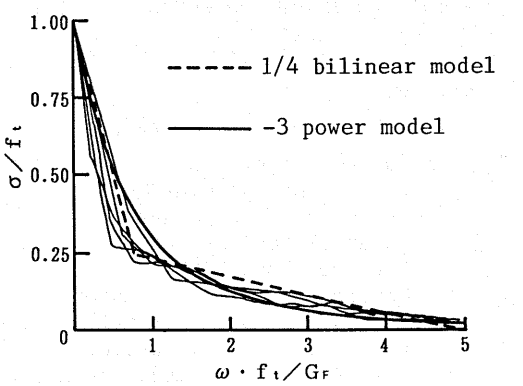

Fig. 28 Normalized tension softening diagrams.

5. CONCLUSIONS

The importance of the measurements of the tension softening diagrams of concrete was pointed out through numerical analysis of the load-displacement curves of concrete beams, where not only the strength properties but also tension softening properties were influential. The Li's J-integral based method and the new J-integral based method to determine tension softening diagrams from bending tests on notched beams were discussed and then the modified J-integral based method was proposed. This modified method has the following features.

(1) In order to determine one softening diagram the Li's method needs data from two beam specimens, whereas the modified method requires data from only one specimen.
(2) In the modified method, the load, the loading point displacement and the crack opening at notch tip are enough to be measured during three-point bending tests on notched beams.
(3) The modified method can be combined with the RILEM method for determination of the fracture energy G_F. So the softening diagram and G_F can be determined at once.
(4) The accuracy of the modified method to determine the softening diagrams is higher than that of the new method, because the second derivative of the potential energy was introduced.

The modified method was applied to various kinds of concrete including high strength concrete, light weight concrete and concrete in early ages. The following results were obtained.

(1) The load-displacement curves of beams were simulated through FE-analysis with the softening diagrams, which were determined through the modified method. Since the simulated curves were in good accordance with the measured ones, the modified method seems to be effective to determine softening diagrams.
(2) The increase in the flexural strength of concrete with age was small as compared with that in the compressive strength and the tensile strength. This can be explained by the small increase in the fracture energy G_F with age.
(3) The shape of the determined tension softening diagrams of the tested concrete were similar to that of the 1/4 bilinear model and the -3 power model.

The size effects on the shape of the tension softening diagrams, if it exists, should be investigated as a further research subject.

REFERENCES

[1] JCI Committee on FMC, "Committee Report on Fracture Mechanics of Concrete", Japan Concrete Institute, JCI-C19, 167p., 1990 (Japanese).
[2] RILEM Draft Recommendation, "Determination of the Fracture Energy of Mortar and Concrete by means of Three-point Bend Tests on Notched Beams", Materials and Structures, Vol.18, No.93, pp.285-290, 1983.
[3] P.E. Petersson, "Crack Growth and Development of Fracture Zone in Plain Concrete and Similar Materials", Report TVBM-1001, Division of Building Materials, Lund Institute of Technology, Sweden, 1981.
[4] F.H. Wittmann, K. Rokugo, E. Brühwiler, H. Mihashi and P. Simonin, "Fracture Energy and Strain Softening of Concrete as Determined by means of Compact Tension Specimens", Materials and Structures, Vol.21, No.121, pp.21-32, 1988.
[5] X.Z. Hu and F.H. Wittmann, "Fracture Process Zone and K_r-curve of Hardened Cement Paste and Mortar", Fracture of Concrete and Rock, Elsevier Applied Science, pp.307-316, 1989.
[6] V.C. Li and R.J. Ward, "A Novel Testing Technique for Post-peak Tensile Behavior of Cementitious Materials", Fracture Toughness and Fracture Energy, Balkema, pp.183-195, 1989.
[7] K. Rokugo, M. Iwasa, S. Seko and W. Koyanagi, "J-integral Approach to Determine Tension Softening Curve of Concrete from Bending Tests", CAJ Proc. of Cement and Concrete, No.43, pp.304-309, 1989 (Japanese).
[8] K. Rokugo, M. Iwasa, T. Suzuki and W. Koyanagi, "Testing Method to Determine Tensile Strain Softening Curve and Fracture Energy of Concrete", Fracture Toughness and Fracture Energy, Balkema, pp.153-163, 1989.
[9] A. Hillerborg, "Stability Problems in Fracture Mechanics Testing, Fracture of Concrete and Rock, Elsevier Applied Science, pp.369-378, 1989
[10] Y. Uchida, T. Suzuki, K. Rokugo and W. Koyanagi, "Determination of Tension Softening Curves by means of Bending Tests", Proc. of JCI Colloquium on Fracture Mechanics of Concrete Structures, JCI-C19, pp.5-12, 1990 (Japanese).